

# Glycerol and Antimicrobial Peptide-Modified Natural Latex for Bacteriostasis of Skin Wounds

Ruonan Wang, Rongyu Li,\* Fangkai Li, Peng Zheng, Zhou Wang, and Senhe Qian\*

Cite This: *ACS Omega* 2023, 8, 1505–1513

Read Online

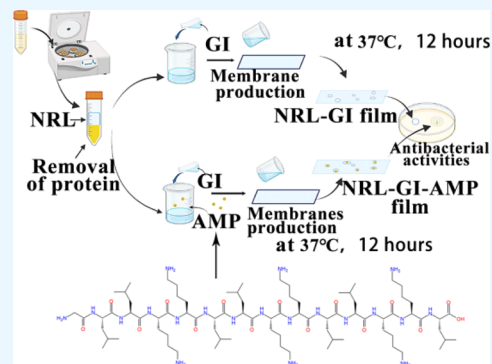
ACCESS |

Metrics &amp; More

Article Recommendations

Supporting Information

**ABSTRACT:** This work aimed to develop a glycerol antimicrobial peptide natural latex film (NRL-GI-AMP film) for the treatment of skin wound infections. The contents of this work mainly include investigating the effect of adding glycerol (GI) and an antimicrobial peptide (AMP) on the physical and chemical properties of natural latex (NRL) and analyzing the cytocompatibility, bacteriostatic activity, and infected wound healing promotion of the NRL-GI-AMP film. The results showed that the addition of GI resulted in more pores in the internal structure of the NRL film, while the addition of G(LLKK)<sub>3</sub>L AMP did not change the structure and properties of the NRL film. Compared with that of the NRL film, the infrared spectrum of the NRL-GI-AMP film did not produce new characteristic peaks, indicating that GI and AMP were non-covalently cross-linked with NRL. Addition of 10% GI reduces the toughness of the NRL-GI-AMP film by 62.0%, increases the water vapor transmission rate by 8.95 mg/(cm<sup>2</sup>·h), and reduces the water absorption and water retention distributions by 33.0 and 24.7%, respectively. AMP in the NRL-GI-AMP film could be released continuously for 40 h, and the release rate was about 45%. The NRL-GI-AMP film showed good biocompatibility and antibacterial activity and promoted the healing of infected wounds. Therefore, the NRL-GI-AP film has potential application in the development of dressings to inhibit skin wound infection and promote wound healing.



## INTRODUCTION

The protective epidermis of a wound will be lost due to skin damage, and pathogenic bacteria can directly enter the wound, resulting in serious infection of the wound and a serious threat to human health.<sup>1</sup> For example, the infection of burns, diabetic foot, and postoperative wounds remains the leading cause of death in patients;<sup>2</sup> in particular, foot ulcers in diabetic patients take a long time to heal, which increases the risk of wound infection.<sup>3,4</sup> The common pathogens of wound infection are *Staphylococcus aureus* (*S. aureus*), *Escherichia coli* (*E. coli*), and other pathogens. The traditional drug for treating bacterial infections is antibiotics, but the long-term use or even abuse of antibiotics has led to the emergence of drug-resistant bacteria.<sup>5,6</sup> Therefore, it is increasingly urgent to find an alternative to antibiotics. Antimicrobial peptides (AMPs) are one of the most potential alternatives.<sup>7</sup> AMPs are polypeptide compounds with a wide range of sources and can be isolated from microorganisms, animals, plants, and even marine organisms.<sup>8</sup> AMPs facilitate pathogenic bacteria develop drug resistance much slower compared to antibiotics, and most AMPs have broad-spectrum antibacterial activity, which not only inhibits bacteria but also inhibits fungi and viruses.<sup>9</sup> In addition, AMPs also have anti-inflammatory, wound healing, and cosmetic functions.<sup>10</sup>

Natural wound healing is usually very slow, which will expose serious wounds to air for a long time and increase the chance of pathogenic infections. Therefore, the use of wound

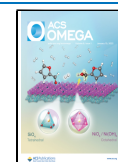
dressings to promote wound healing is currently a commonly used method.<sup>11</sup> In order to promote wound healing rapidly, it is necessary to develop wound dressings with antibacterial and anti-inflammatory activities, biocompatibility, and skin friendliness.

Natural latex (NRL) is a liquid compound secreted by *Hevea oleifera*, and it is extremely easy to obtain in the region where rubber trees are grown.<sup>12</sup> NRL is mainly composed of long poly-chain (*cis*-1,4-polyisoprene) particles, which accounts for more than 90% of its content; it also contains some other substances, such as proteins and fatty acids.<sup>13</sup> At present, the application of NRL has entered various parts of people's life, such as latex gloves, latex headrests, latex mattresses, and so forth.<sup>14,15</sup> NRL is a material with good biocompatibility that not only possesses tissue repair properties but also acts as a solid carrier for compounds with pharmacological activities.<sup>16,17</sup> In addition, NRL has good film-forming properties, but its wide application in films is limited due to its stronger elasticity and higher compactness.<sup>18</sup> Therefore, a plasticizer is

Received: October 31, 2022

Accepted: December 16, 2022

Published: December 28, 2022



needed to improve its tensile and structural properties. Glycerol, also known as glycerin (GI), is not only used in the cosmetic industry<sup>19</sup> but also used as a plasticizer to improve the mechanical properties of polymer materials to obtain better flexibility.<sup>20</sup> Previous literature has reported that adding GI to NRL can increase the flexibility and wettability of latex films.<sup>21</sup> In addition, GI, as a plasticizer, can increase the porosity of the internal structure of the polymer material film. Mbituyimana *et al.*<sup>22</sup> added GI to the bacterial cellulose film, and the fibrous structure of the film became looser and had more pores, which provides favorable conditions for the effective release of the drug in the polymer material film.

In this study, GI was used to modify NRL to prepare a glycerol natural latex film (NRL-GI film) to reduce its elasticity, increase its porosity, and improve the performance of the film dressing.<sup>23</sup> At the same time, G(LLKK)<sub>3</sub>L AMP was added to the NRL-GI film to develop a glycerin antibacterial peptide film (NRL-GI-AMP film) with antibacterial and wound healing functions.<sup>12,24</sup>

## EXPERIMENTAL SECTION

**Synthesis of an AMP.** G(LLKK)<sub>3</sub>L AMP was synthesized by the solid-phase method.<sup>25</sup> The synthesized product was separated by reversed-phase high-performance liquid chromatography (RP-HPLC, Jiangsu Hanbon Science & Technology Co., Ltd.) on a C18 preparative column (30 mm × 250 mm).

**Synthesis of the NRL-GI-AMP Film.** NRL was placed in a centrifuge tube and centrifuged at 12,000 rpm for 10 min. After centrifugation, the precipitation at the bottom was removed to reduce allergic reactions caused by high-molecular-weight proteins.<sup>26</sup> After three times of centrifugation, a relatively stable and pure NRL colloid component was obtained. GI and NRL were mixed according to the volume ratios of 0, 5, 10, 15, and 20% and shaken well using a mixer, and then 2 mL of the mixture was added to a 7.5 cm × 1.6 cm mold. After drying in an oven at 37 °C for 12 h, the tensile properties were measured by a texture analyzer (GT3 texture analyzer; Brookfield, USA), and the effect of GI addition on the tensile properties of the NRL films was evaluated. On the basis of optimizing the ratio of GI addition, the effect of G(LLKK)<sub>3</sub>L AMP addition on the tensile properties of the NRL-GI-film was further analyzed; that is, the NRL-GI-AMP film with G(LLKK)<sub>3</sub>L AMP concentrations of 0, 200, 600, 800, 1200, and 1600 μg/mL was prepared, and the tensile properties were measured.

**Cytotoxicity Analysis.** The NRL-GI-AMP film-forming solution with G(LLKK)<sub>3</sub>L AMP concentrations of 0, 200, 600, 800, 1200, and 1600 μg/mL was prepared, and 50 μL of the film-forming solution was dropped on a glass plate to prepare the NRL-GI-AMP film and ultraviolet-sterilized after drying. The sterilized NRL-GI-AMP film was then transferred to a sterile 96-well plate, and 200 μL of the MEF cell suspension (about 5000 cells) was added and then placed in a carbon dioxide cell incubator for culture. After 12 h, 20 μL of the CCK-8 reagent was added, and after shaking, it was placed in a carbon dioxide cell incubator for 4 h. Then, the NRL-GI-AMP film was taken out from the 96-well plate, and the absorbance at 450 nm was measured with a microplate reader.<sup>27</sup> The cell viability is calculated by eq 1.

$$\text{Cell viability} = \frac{[\text{OD}(x) - \text{OD}(0)]}{[\text{OD}(N) - \text{OD}(0)]} \times 100\% \quad (1)$$

where OD(x) is the absorbance of the mixture of the MEF cell suspension (the NRL-GI-AMP film at the bottom of the wells) and the CCK-8 solution, OD(0) is the absorbance of the mixture of the culture medium (no NRL-GI-AMP film at the bottom of the wells) and the CCK-8 solution, and OD(N) is the absorbance of the mixture of the culture medium (the NRL-GI-AMP film at the bottom of the well) and the CCK-8 solution.

**Hemolytic Activity Analysis.** The hemolytic activity was analyzed according to Wang *et al.*<sup>28</sup> Defibrillated sheep blood cells (2 mL) were centrifuged at 1000 rpm for 10 min, and the supernatant was discarded. The precipitate was washed and centrifuged several times by adding PBS until the supernatant did not show red color. PBS was used to prepare a 2% (v/v) red blood cell solution. A NRL-GI-AMP film of 1 cm<sup>2</sup> was immersed in 1 mL of PBS for 12 h. The leaching solution was mixed with the 2% red blood cell solution at 1:1 (v/v) and left at room temperature for 3 h, followed by centrifugation at 1000 rpm for 10 min. The deionized water group was used as the positive control and the PBS group as the negative control.

**Determination of the Water Vapor Transmission Rate, Water Absorption Rate, and Water Retention Rate.**

The water vapor transmission rate ( $W_{vp}$ ) was determined using the method reported by Abbasi *et al.*<sup>29</sup> Deionized water (10 mL) was added to a conical flask with a diameter of 2 cm at the mouth (the area of the bottle mouth is  $S$ ), and the bottle mouth was wrapped with the prepared NRL film, NRL-GI film, and NRL-GI-AMP film, and the total mass ( $m_0$ ) was measured. The total mass ( $m_{12}$ ) was measured again after placing it in a 37 °C oven for 12 h, and  $h$  was 12 h. The water vapor transmission rate ( $W_{vp}$ ) is calculated by eq 2.

$$W_{vp} = \frac{m_{12} - m_0}{S \times h} \quad (2)$$

The water absorption and water retention rates of the films were determined using the method of Sun *et al.*<sup>30</sup> The NRL film, NRL-GI film, and NRL-GI-AMP film were prepared; the films were cut into 1 cm × 1 cm specifications and dried at 40 °C to a constant weight. Their mass was determined as  $W_0$ . The films were soaked in deionized water for 60 min, and then filter paper was used to absorb free water on the surface. Their mass was determined as  $W_{60}$ . The films were then placed in a centrifuge tube with a filter screen and centrifuged at 3500 rpm for 3 min, and their mass was determined as  $W_c$ .

The water absorption ( $W_a$ ) and water retention ( $W_r$ ) rates are calculated by eqs 3 and 4, respectively.

$$W_a = \frac{(W_{60} - W_0)}{W_0} \times 100\% \quad (3)$$

$$W_r = \frac{W_c - W_0}{W_{60} - W_0} \times 100\% \quad (4)$$

**Analysis of Thermal and pH Stabilities of Tensile Properties.** The NRL-GI-AMP film was exposed to different temperatures (−20, 4, 20, 30, 40, 50, and 60 °C) and different pH values (4, 5, 6, 7, 8, 9, and 10) for 24 h, respectively, and the tensile properties were measured.

**AMP Release in the NRL-GI-AMP Film.** The concentration of G(LLKK)<sub>3</sub>L is taken as the abscissa, measurement of its absorbance at 229 nm is taken as the ordinate, and the AMP standard curve is drawn. The NRL-GI-AMP film was put into sterile water, the absorbance was measured at regular intervals,

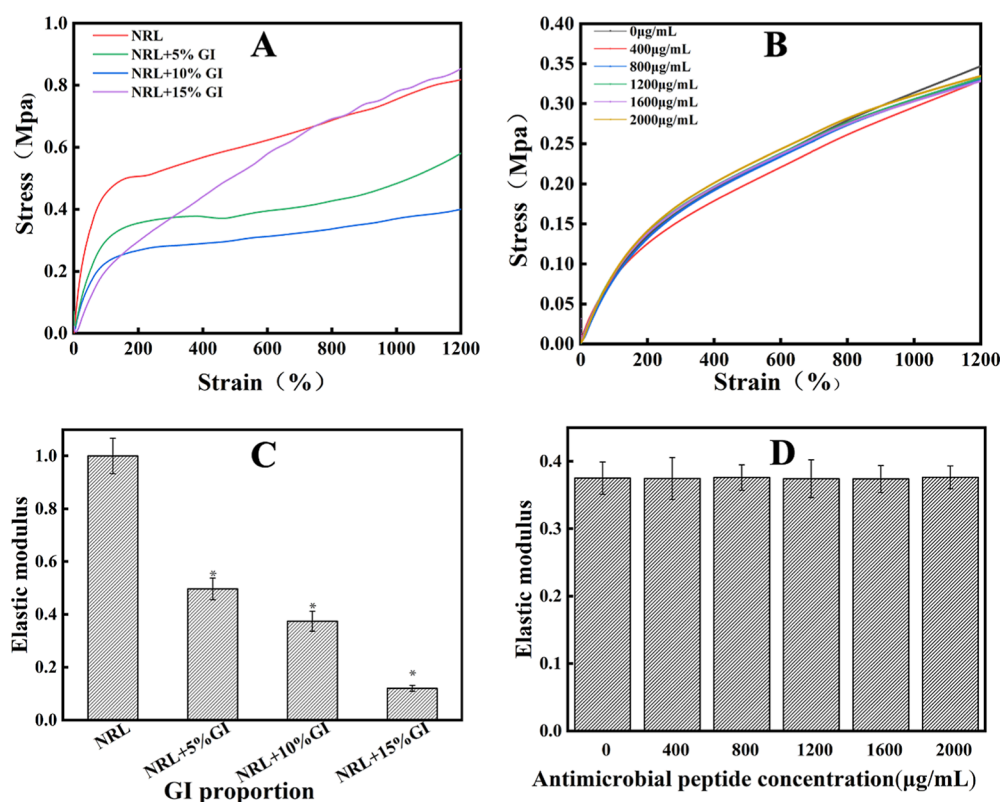


**Figure 1.** Effects of GI and AMP additions on the tensile properties of NRL films. (A) Stress–strain curve of the NRL-GI film, (B) stress–strain curve of the NRL-GI-AMP film, (C) Young's modulus of the NRL-GI film, and (D) Young's modulus of the NRL-GI-AMP film. \*indicates a significant difference ( $p < 0.05$ ).

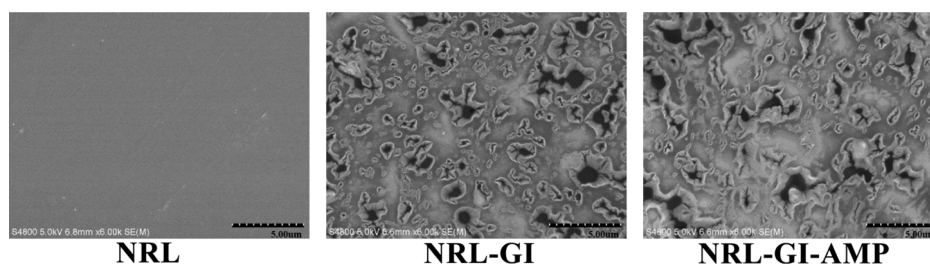


**Figure 2.** SEM images of the NRL film, NRL-GI film, and NRL-GI-AMP film.

an equal amount of phosphate buffer was added after each suction, the amount of AMP released at different times was calculated according to the standard curve, and the AMP release curve was drawn.

**Inhibition Zone Test.** A NRL-GI-AMP film with a  $G(LLKK)_3L$  concentration of  $600 \mu\text{g/mL}$  was prepared, and a round film with a diameter of 7 mm was cut with a hole punch. After ultraviolet sterilization, the plate method was used to conduct the inhibition zone experiment to observe and analyze the antibacterial effect of the NRL-GI-AMP film on *S. aureus* and *E. coli*.

**PI Flow Analysis.** *S. aureus* and *E. coli* cell suspensions in the logarithmic growth phase were treated with the leaching solution obtained by soaking the NRL-GI-AMP film for 40 h, and the concentration of the cells was controlled to be  $10^4$ – $10^5$  cfu. The NRL-GI-AMP film leaching solution was used as the experimental group, and PBS was used as the control group. The cells were collected and stained with PI for 10 min in the dark, and the number of dead and viable cells was

determined using a CytoFLEX flow analyzer (Beckman-Coulter).

**In Vivo Experiments.** C57BL/6 black male mice ( $26 \pm 2$  g) were obtained from the Nanjing Qinglongshan Animal Breeding Farm (Nanjing, China) and housed under standard environmental conditions ( $22 \pm 2$  °C,  $55 \pm 5\%$  humidity, and 12 h dark/light cycle each). All animals were housed according to the guidelines outlined in the “Guide for the Care and Use of Laboratory Animals”. All animal experiments were approved by the Wannan Medical College (Wuhu, China) Animal Care (approval number: 2021-LLSC-047). The hair on the back of each experimental mouse was shaved off, and a shallow wound with an area of about  $1.0 \text{ cm}^2$  was cut. *S. aureus* ( $200 \mu\text{L}$ ,  $10^5$  cfu/mL) was inoculated to the wounds of mice for infection, and the wounds were wrapped with gauze to prevent mice licking each other's wounds. After the wounds get infected, they were wrapped with the NRL-GI-AMP film as the experimental group, the NRL-GI film as the control group, and gauze as the blank group (the wound was smeared with

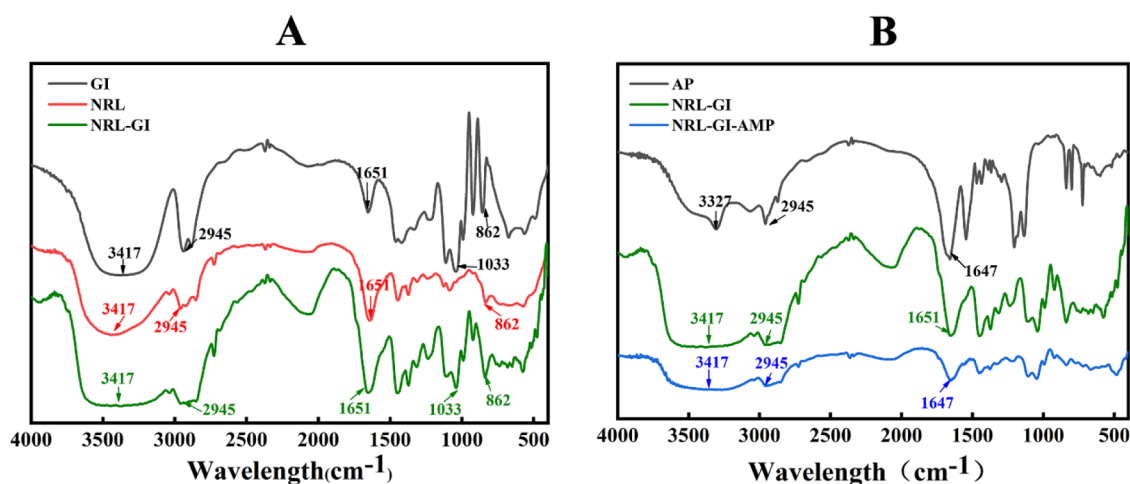


Figure 3. FTIR of (A) GI, NRL, and NRL-GI. (B) AMP, NRL-GI, and NRL-GI-AMP.

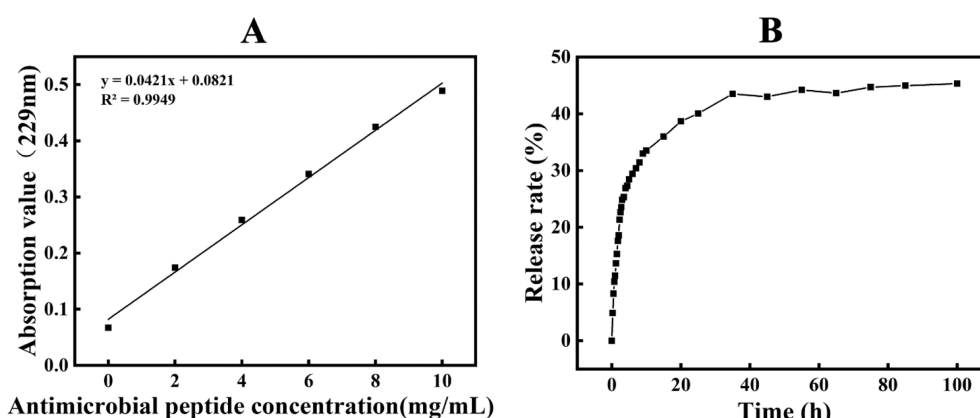


Figure 4. (A) Plots of AMP concentration and absorbance and (B) release profiles of AMP in the NRL-GI-AMP film.

150  $\mu\text{L}$  of PBS). Each group includes three parallels. The wound images were obtained every 2 days.

## RESULTS AND DISCUSSION

**Effect of GI Addition on the Morphology of the NRL-GI Film.** To investigate the effect of GI addition on the surface morphology of NRL-GI films, the surfaces of the films with GI contents of 5, 10, 15, and 20% were compared with the films without GI addition, as shown in Figure S1 (in the Supporting Information). With the increase of the GI ratio, the NRL-GI

film gradually changes from the transparent state to an opaque light-yellow color. When the GI ratio was 15 and 20%, the morphology of the film changed obviously, its surface became uneven, and liquid GI was precipitated, indicating that the GI carried by the NRL film was close to saturation. The results are similar to those of the previous reports by Ghasemlou *et al.*<sup>31</sup> using GI to plasticize the Kefiran Gum (kefir polysaccharide) degradable film. Hydrogen bonds can be formed between the  $-\text{OH}$  of the plasticizer molecules and the  $-\text{COOH}$  and  $-\text{OH}$  of the film material, thereby weakening the force between the molecular chains of the film material and improving the mobility of their molecular chains, but higher concentrations of plasticizers can affect the cross-linking among the molecules of the film material, leading to a decrease in its film-forming properties.<sup>32</sup>

**Effects of GI and AMP Additions on the Tensile Properties of NRL-GI Films.** As a plasticizer, GI can affect the stability of the internal structure of polymer materials, resulting in changes in tensile strength.<sup>33</sup> With the increase of the GI ratio, the Young's modulus of the NRL-GI film gradually decreases, as shown in Figure 1A,C, indicating that the softness of the NRL-GI film gradually increases. When the GI ratio is less than 10%, the morphological characteristics of the NRL-GI film are relatively stable, and the tensile force is easier to be measured. However, when the proportion of GI is more than 15%, the NRL-GI film becomes unstable and too soft to measure its tensile force. Therefore, it is more

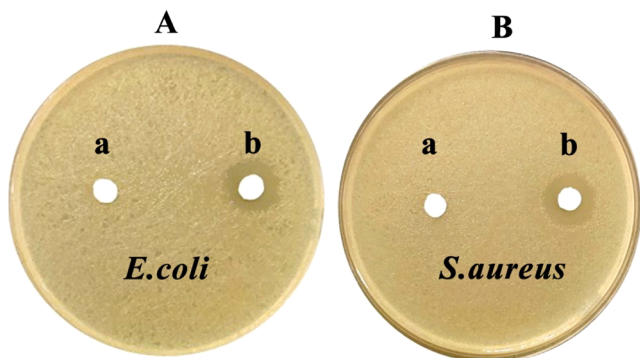


Figure 5. Inhibition zone of the NRL-GI-AMP film. (A,B) are the inhibition zones of *E. coli* and *S. aureus*, respectively; a and b show the NRL-GI and NRL-GI-AMP films, respectively.

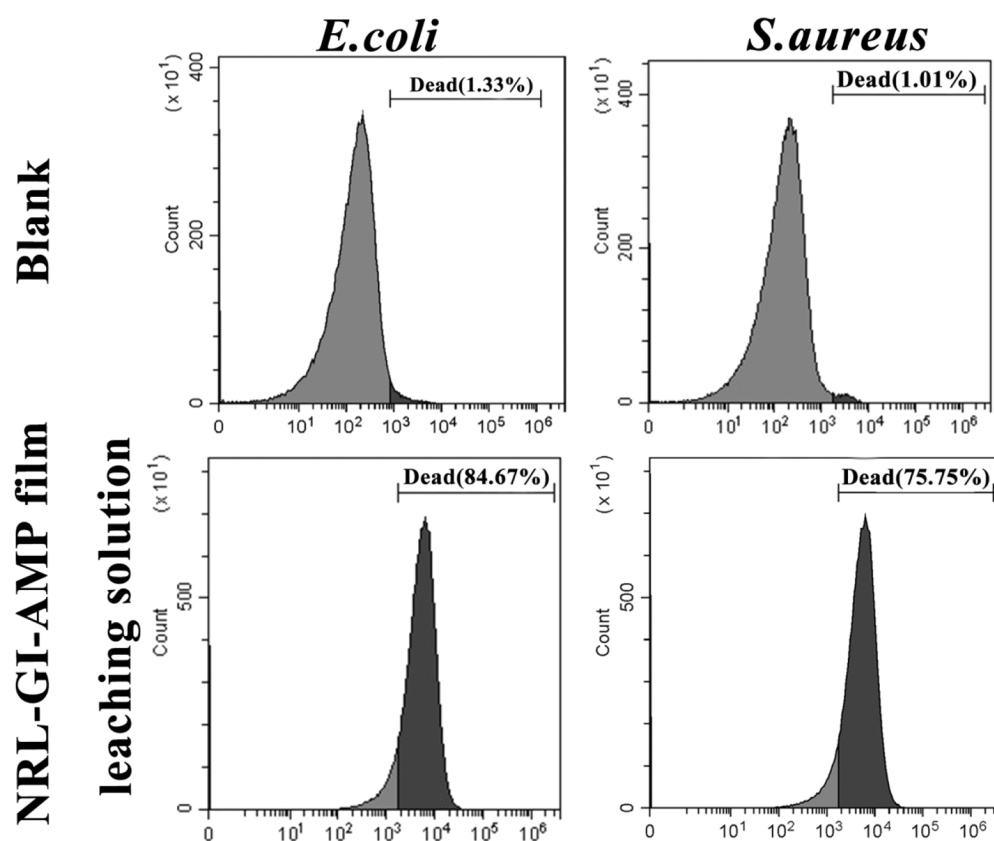


Figure 6. Effect of the NRL-GI-AMP film leaching solution on the viability of *E. coli* and *S. aureus* cells.

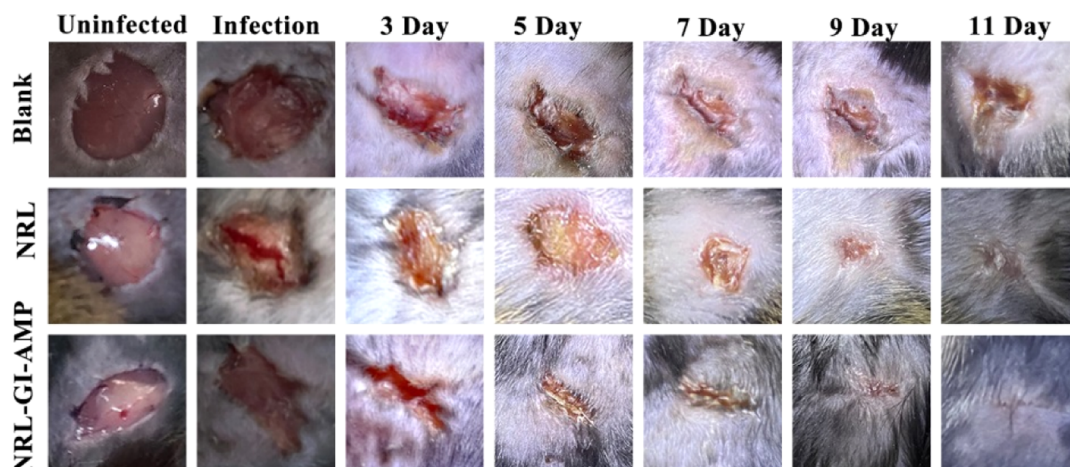


Figure 7. Healing effect of the NRL-GI-AMP film on the infected wound.

appropriate to add 10% GI. Previous studies have shown that GI can improve the tensile properties of  $\gamma$ -glutamic acid ( $\gamma$ -PGA) gellan gum-based films, but a very high proportion of GI addition will reduce the tensile strength, elastic modulus, and elongation at break of the films.<sup>34</sup> The results show that adding an appropriate amount of GI help to reduce the toughness of the polymer material and improve its tensile properties.

In contrast, the addition of G(LLKK)<sub>3</sub>L AMP to the NRL-GI film did not significantly change its tensile force curve and Young's modulus, indicating that the addition of the AMP had little effect on the tensile properties of the NRL-GI film (Figure 1B,D).

**Cytotoxicity of the NRL-GI-AMP Film.** Although AMPs have a certain killing effect on pathogenic bacteria, excessive AMP concentrations tend to be toxic to mammalian cells.<sup>35</sup> Therefore, in the NRL-GI-AMP film, if the G(LLKK)<sub>3</sub>L AMP concentration is too high, it will lead to cytotoxicity, and if the AMP concentration is too low, the film cannot achieve a good bacteriostatic effect. When the AMP concentration in the film-forming solution of the NRL-GI-AMP film is lower than 600  $\mu\text{g/mL}$ , the MEF cell activity of the film remains above 80%, and when the AMP concentration is higher than 600  $\mu\text{g/mL}$ , the cell viability is lower than 70%, so it is more appropriate to add 600  $\mu\text{g/mL}$  AMP to the NRL-GI film. The data are shown in Figure S2.

**Hemolysis of the NRL-GI-AMP Film.** The release of hemoglobin can be used to evaluate the damage of the cell membrane caused by materials.<sup>36</sup> The hemolytic activity of the NRL-GI-AMP film on sheep blood cells was investigated as shown in Figure S3. The results showed that the red color of the positive control indicated that hemolysis occurred, while the transparent and colorless states of the negative control indicated that no hemolysis occurred. Therefore, it can be seen that the NRL-GI-AMP film leaching solution did not show hemolysis, indicating that it did not damage the erythrocyte membrane and had a good cytocompatibility.

**Water Vapor Transmission Rate, Water Absorption Rate, and Water Retention Rate of the Films.** The water vapor transmission, water absorption, and water retention rates of several film materials were tested, and the calculation results are listed in Table S1 and Figure S4. It can be seen from Table S1 that the water vapor transmission rate of the NRL film is relatively low, indicating that its surface structure is relatively tight and water vapor is not easily permeable, while the water vapor transmission rates of NRL-GI and NRL-GI-AMP films are relatively high, increased by 318.87 and 337.74%, respectively, compared with the control group. This may be due to the decrease in the compactness of the film after GI modification, which increases the air permeability and facilitates the permeation of water vapor.<sup>37</sup> Therefore, if the GI-modified NRL film is used as a wound dressing, it is more conducive to wound ventilation and promotes wound healing.<sup>38</sup>

At the same time, the addition of GI has a positive effect on the water absorption of the NRL film (Figure S4A). The water absorption rate of NRL-GI and NRL-GI-AMP films was significantly lower than that of the NRL film, which may be due to the addition of GI which loosens the internal structure of the NRL film, resulting in a decrease in the water absorption rate of the film.<sup>39</sup> The reduced water absorption can reduce the swelling of the film and prolong its service life.<sup>29</sup> Similarly, Figure S4B shows that the water retention rate of NRL-GI and NRL-GI-AMP films is also significantly lower than that of the NRL film, which may also be related to the loosening the film structure by GI. The lower water retention rate is beneficial to the discharge of sweat after the film acts on the skin, which increases the comfort of the skin.<sup>40</sup> In addition, it can be seen that the addition of an AMP has no obvious effect on the water vapor transmission, water absorption, and water retention rates of the NRL-GI film.

**SEM Image of the Films.** Before adding GI and the AMP, the surface of the NRL film is smooth, compact, and without obvious pores (Figure 2A), which is consistent with the result of Silva *et al.*<sup>41</sup> that there are no pores on the surface of the NRL film. Figure 2B,C shows the SEM images of NRL-GI and NRL-GI-AMP films, respectively. It can be clearly seen that there are many pores with different sizes on the surface of NRL-GI and NRL-GI-AMP films, indicating that the addition of GI can change the compactness of the NRL film structure. The reason may be that a hydrogen bond is formed between the  $-\text{COOH}$  of the protein and the  $-\text{OH}$  of GI in NRL, which loosens the structure of the NRL film, resulting in more pores in its surface structure.<sup>16,42</sup> In addition, there was no significant difference in the surface structure of NRL-GI and NRL-GI-AMP films, indicating that the addition of G-(LLKK)<sub>3</sub>L AMP did not significantly affect the compactness of the NRL-GI film.

**FTIR of the Films.** As shown in Figure 3A, there are five peaks at 3417, 2945, 1651, 1033, and 862  $\text{cm}^{-1}$  in the GI infrared spectrum, which are attributed to the stretching vibration of  $-\text{OH}$ , the contraction vibration of  $-\text{CH}_2$  and the C–C bond, the stretching vibration of the C–O bond, and the stretching vibration of the  $-\text{CH}$  bond, respectively. The same five peaks appeared in the NRL film, but no obvious C–O peak appeared at 1033  $\text{cm}^{-1}$ . The above five peaks appeared in the NRL-GI film, and the broad peak at 3417  $\text{cm}^{-1}$  may be attributed to the vibration of the binding of  $-\text{COOH}$  of protein in NRL and  $-\text{OH}$  in GI.<sup>43</sup> Normally, when the two substances are covalently bound and chemically reacted, additional absorption peaks will appear,<sup>44</sup> but no new infrared absorption peaks appeared on the NRL-GI film, indicating that GI and NRL may be non-covalently bound.

From the infrared spectra of AMP, NRL-GI, and NRL-GI-AMP films in Figure 3B, it can be seen that the characteristic absorption peak of AMP has a N–H peak at 3327  $\text{cm}^{-1}$ , and the amide I band at 1647  $\text{cm}^{-1}$  appears. In the infrared spectra of NRL-GI and NRL-GI-AMP films, the peaks at 2945 and 1651  $\text{cm}^{-1}$  are caused by the stretching vibration of  $-\text{CH}_2$  and the stretching vibration of the C–C bond, respectively. A broad peak appeared at 3417  $\text{cm}^{-1}$ , which may be caused by the binding of  $-\text{COOH}$  of the protein in NRL and  $-\text{OH}$  in GI; additionally, the N–H in the AMP binds to the  $-\text{COOH}$  of the protein, which also leads to the emergence of wide peaks. The characteristic peak of AMP also appears in the NRL-GI-AMP film, and the position does not shift, indicating that there is no covalent binding between the AMP and NRL-GI-films.

**Thermal Behavior of the Films.** As shown in Figure S5, the mass loss of the three films occurred from about 30 to 150  $^{\circ}\text{C}$ , which may be the evaporation rate of free water in the free state. From 150 to 330  $^{\circ}\text{C}$ , NRL-GI film has a mass loss of about 22%, and the NRL-GI-AMP film has a mass loss of about 18%. The reason is that GI is a polyhydroxy organic matter that is more easily evaporated.<sup>42</sup> The mass loss of the three films was obvious after 330  $^{\circ}\text{C}$ , which may be caused by the scission of the main chain of NRL.<sup>45</sup> However, when the degradation amount is the same, the temperature tolerance of NRL-GI-AMP and NRL-GI films is lower than that of the NRL film. It may be due to the addition of GI that makes the NRL-GI and NRL-GI-AMP films non-resistant to high temperature and easy to age.<sup>46</sup> In addition, the AMP in the NRL-GI-AMP film is a protein with a short-chain structure and has an antiaging effect, so the heat resistance of the NRL-GI-AMP film is higher than that of the NRL-GI film.<sup>47</sup> Zhan *et al.*<sup>48</sup> reported that the addition of soy protein to natural rubber can promote the construction of a vulcanization network, increase the rigidity of the rubber, and reduce the breakage of the rubber chain.

**Effect of Temperature and pH on the Tensile Properties of the NRL-GI-AMP Film.** It can be seen from Figure S6A,C that the temperature is too low or too high to have a certain influence on the tensile properties of the NRL-GI-AMP film. The Young's modulus of the NRL-GI-AMP film changes slightly when the temperature range is 20–40  $^{\circ}\text{C}$ , indicating that its tensile properties are relatively stable in this temperature range. Under freezing conditions, latex can agglomerate, resulting in an increased mechanical tension,<sup>49</sup> while higher temperature may cause the GI in the NRL-GI-AMP film to migrate and exude, which also leads to increased mechanical tension.

With the increase of pH, the Young's modulus of the NRL-GI-AMP film first increased and then decreased, indicating that its mechanical tensile force first increased and then decreased (Figure S6B,D). When the pH was 9.0, its mechanical tensile force is the largest, and when the pH is between 6.0 and 8.0, its tensile properties are relatively stable. The main component of NRL is *cis*-1,4-polyisoprene, which has obvious C=C bonds and is prone to a halogenation reaction under acidic conditions, resulting in insufficient stability of the NRL-GI-AMP film.<sup>50</sup> Weak bases can generally be used as stabilizers for NRL, but under the condition of strong bases, the protective layer of colloidal particles in NRL films will be damaged and the stability of colloidal particles will be reduced.<sup>51</sup>

**Release of AMP from the NRL-GI-AMP Film.** Figure 4A shows the standard curve of AMP concentration and the  $A_{229}$  nm absorption value, and its regression equation is  $y = 0.0421x + 0.0821$ ; the release rate of AMP can be calculated according to the regression equation. In the NRL-GI-AMP film, the release speed of AMP was faster in the first 10 h, and the release rate was about 30%; in 10–40 h, the release speed of AMP in the NRL-GI-AMP film was significantly slowed down; and after 40 h, the AMP release rate tends to be stable, which is about 45% (Figure 4B). This result indicates that the AMP in the NRL-GI-AMP film can be released slowly. Romeiro Miranda *et al.*<sup>39</sup> reported that the release rate of bovine serum albumin reached 88% in the NRL film after 12 h. In addition, Silva *et al.* reported that the release rate of voriconazole in the NRL film reached 24.2% after 48 h. These results confirmed that the NRL film is feasible as a drug-loaded sustained release carrier, but different drugs have different release properties.

**Antibacterial Properties of the NRL-GI-AMP Film.** The ideal drug carrier is that the drug contained in it can be released slowly and exerts corresponding pharmacological effects. For example, NRL dressings loaded with voriconazole, which can release voriconazole slowly and efficiently, are used in the treatment of skin ulcers with candida infection.<sup>41</sup> It can be seen from Figure 5 that the NRL-GI film had no inhibitory effect on *E. coli* and *S. aureus* and did not produce an inhibition zone, while the NRL-GI-AMP film had the inhibition zone with different sizes against *E. coli* and *S. aureus*. It can be proved that AMP can be effectively released from the NRL-GI-AMP film to exert its antibacterial activity.

**Killing Effect of the NRL-GI-AMP Film Leaching Solution on Bacterial Cells.** In order to further detect the killing effect of the NRL-GI-AMP film on *E. coli* and *S. aureus* cells, the uptake of PI by cells treated with the NRL-GI-AMP film leaching solution was analyzed by flow cytometry. PI cannot cross live cell membranes but can cross the cell membranes of late apoptosis and dead cells and stain its nuclei with red fluorescence. Therefore, the proportion of dead and live cells can be analyzed by flow cytometry.<sup>52,53</sup> It can be seen from Figure 6 that the NRL-GI-AMP film leaching solution has a greater killing effect on *S. aureus* with a mortality rate of 75.75% while that of *E. coli* is 84.67%. Thus, we can see that the leaching solution of the NRL-GI-AMP film has a strong bactericidal activity on *E. coli* and *S. aureus*.

**Healing Effect of the NRL-GI-AMP Film on Infected Wound.** A wound model of mice infected with *S. aureus* was constructed to demonstrate the role of the NRL-GI-AMP film in promoting healing of infected wounds *in vivo*, and the results are shown in Figure 7. It can be seen from Figure 7 that after 3 days of treatment with the NRL-GI-AMP film, the wound infection disappeared and the wound area decreased

significantly; however, for the NRL-GI film group and the blank group, the wounds were still seriously infected. When treated with the NRL-GI-AMP film for 11 days, the wound was almost completely healed, but for the NRL-GI film group and the blank group, the infection persisted despite the reduced wound area.

## CONCLUSIONS

In this work, the improvement of GI on the NRL film performance is first investigated. The results show that GI can not only improve the toughness of the NRL film, make it have suitable softness, and overcome the shortcomings of poor mechanical properties of hydrogel dressings but also increase the porosity of the NRL film and improve its water vapor transmission rate, water retention, and water absorption properties to ensure the comfort when it acts on the skin. Second, we used an AMP to enhance the antibacterial properties of the NRL-GI film. Thanks to the fact that the AMP in the NRL-GI-AMP film is not covalently bound to the latex, the AMP in the film has better sustained-release performance, and the use of AMPs to replace antibiotics can effectively solve the problem of antibiotic resistance. Moreover, the appropriate concentration of the AMP in the film can make the NRL-GI-AMP film have good biocompatibility and promote antibacterial and infected wound healing properties. In conclusion, this study demonstrates that the NRL-GI-AMP film has excellent properties as a wound dressing and can effectively inhibit bacterial infection of wounds.

## ASSOCIATED CONTENT

### Supporting Information

The Supporting Information is available free of charge at <https://pubs.acs.org/doi/10.1021/acsomega.2c07008>.

Chemicals, materials, apparatus, surface morphology, cytotoxicity, water absorption, water retention, TGA, stress–strain curves, hemolytic activity, and Young's modulus (PDF)

## AUTHOR INFORMATION

### Corresponding Authors

Rongyu Li – School of Basic Medical Sciences, Wannan Medical College, Wuhu 241002, China;  
Email: [lirongyu\\_2000@163.com](mailto:lirongyu_2000@163.com)

Senhe Qian – College of Biological and Food Engineering, Anhui Polytechnic University, Wuhu 241000, China;  
[orcid.org/0000-0003-0624-3081](https://orcid.org/0000-0003-0624-3081); Email: [qiansenhe@163.com](mailto:qiansenhe@163.com)

### Authors

Ruonan Wang – College of Biological and Food Engineering, Anhui Polytechnic University, Wuhu 241000, China  
Fangkai Li – College of Biological and Food Engineering, Anhui Polytechnic University, Wuhu 241000, China  
Peng Zheng – College of Biological and Food Engineering, Anhui Polytechnic University, Wuhu 241000, China  
Zhou Wang – College of Biological and Food Engineering, Anhui Polytechnic University, Wuhu 241000, China

Complete contact information is available at:  
<https://pubs.acs.org/10.1021/acsomega.2c07008>

## Author Contributions

The manuscript was written through contributions of all authors. All authors have given approval to the final version of the manuscript.

## Notes

The authors declare no competing financial interest.

## ACKNOWLEDGMENTS

This work was financially supported by the Scientific Research Project of Colleges and Universities in Anhui Province (nos. KJ2021A0840, YJS20210451, and KJ2020A0374).

## ABBREVIATIONS

AMP, antimicrobial peptide; NRL, natural latex; GI, glycerol; NRL-GI, glycerol natural latex film; NRL-GI-AMP, glycerol antimicrobial peptide natural latex film; MEF, mouse embryonic fibroblast; PI, propidium iodide; SEM, scanning electron microscopy; FTIR, Fourier transform infrared spectrometry; TGA, thermogravimetric analysis; *S. aureus*, *Staphylococcus aureus*; *E. coli*, *Escherichia coli*

## REFERENCES

- (1) von Müller, C.; Bulman, F.; Wagner, L.; Rosenberger, D.; Marolda, A.; Kurzai, O.; Eißmann, P.; Jacobsen, I. D.; Perner, B.; Hemmerich, P.; Vylkova, S. Active Neutrophil Responses Counteract *Candida albicans* Burn Wound Infection of Ex Vivo Human Skin Explants. *Sci. Rep.* **2020**, *10*, 21818.
- (2) Young, A. E.; Thet, N. T.; Mercer-Chalmers, J.; Greenwood, R. J.; Coy, K.; Booth, S.; Sack, A.; Jenkins, A. T. A. The SPaCE Diagnostic: A Pilot Study to Test the Accuracy of a Novel Point of Care Sensor for Point of Care Detection of Burn Wound Infection. *J. Hosp. Infect.* **2020**, *106*, 726–733.
- (3) Alven, S.; Peter, S.; Mbese, Z.; Aderibigbe, B. A. Polymer-Based Wound Dressing Materials Loaded with Bioactive Agents: Potential Materials for the Treatment of Diabetic Wounds. *Polymers* **2022**, *14*, 724.
- (4) Yan, Y.; Liu, X.; Zhuang, Y.; Zhai, Y.; Yang, X.; Yang, Y.; Wang, S.; Hong, F.; Chen, J. Pien Tze Huang Accelerated Wound Healing by Inhibition of Abnormal Fibroblast Apoptosis in Streptozotocin Induced Diabetic Mice. *J. Ethnopharmacol.* **2020**, *261*, 113203.
- (5) Mei, L.; Zhang, D.; Shao, H.; Hao, Y.; Zhang, T.; Zheng, W.; Ji, Y.; Ling, P.; Lu, Y.; Zhou, Q. Injectable and Self-Healing Probiotics-Loaded Hydrogel for Promoting Superbacteria-Infected Wound Healing. *ACS Appl. Mater. Interfaces* **2022**, *14*, 20538–20550.
- (6) Cao, M.; Wang, S.; Hu, J. H.; Lu, B. H.; Wang, Q. Y.; Zang, S. Q. Silver Cluster-Porphyrin-Assembled Materials as Advanced Bioprotective Materials for Combating Superbacteria. *Adv. Sci.* **2022**, *9*, No. e2103721.
- (7) Ajingi, Y. S.; Muhammad, A.; Khunrae, P.; Rattanarojpong, T.; Pattanapanyasat, K.; Sutthibutpong, T.; Jongruja, N. Antibacterial Potential of a Novel Peptide from the Consensus Sequence of Dermaseptin Related Peptides Secreted by *Agalychnis Annae*. *Curr. Pharm. Biotechnol.* **2021**, *22*, 1216–1227.
- (8) Huan, Y.; Kong, Q.; Mou, H.; Yi, H. Antimicrobial Peptides: Classification, Design, Application and Research Progress in Multiple Fields. *Front. Aquat. Microbiol.* **2020**, *11*, 582779.
- (9) Luong, H. X.; Thanh, T. T.; Tran, T. H. Antimicrobial Peptides-Advances in Development of Therapeutic Applications. *Life Sci.* **2020**, *260*, 118407.
- (10) Al-Shammery, K. A.; Hozzein, W. N. Antibacterial Activities of Two Potential Peptides Extracted from *Polistes Wattii* Cameron, 1900 (Vespidae: Polistinae) Wasp Venom Collected at Eastern Province, Saudi Arabia. *PLoS One* **2022**, *17*, No. e0264035.
- (11) Chen, S.; Wang, H.; Jian, Z.; Fei, G.; Qian, W.; Luo, G.; Wang, Z.; Xia, H. Novel Poly(vinyl alcohol)/Chitosan/Modified Graphene Oxide Biocomposite for Wound Dressing Application. *Macromol. Biosci.* **2020**, *20*, No. e1900385.
- (12) Guerra, N. B.; Sant'Ana Pegorin, G.; Boratto, M. H.; de Barros, N. R.; de Oliveira Graeff, C. F.; Herculano, R. D. Biomedical Applications of Natural Rubber Latex from the Rubber Tree *Hevea Brasiliensis*. *Mater. Sci. Eng., C* **2021**, *126*, 112126.
- (13) Dai, L.; Yang, H.; Zhao, X.; Wang, L. Identification of Cis Conformation Natural Rubber and Proteins in *Ficus Altissima* Blume Latex. *Plant Physiol. Biochem.* **2021**, *167*, 376–384.
- (14) Sriring, M.; Nimpaiboon, A.; Kumarn, S.; Srisinha, C.; Sakdapianich, J.; Toki, S. Viscoelastic And Mechanical Properties of Large-and Amall-Particle Natural Rubber before and after Vulcanization. *Polym. Test.* **2018**, *70*, 127–134.
- (15) Qu, W.; Zhu, Y.; Huang, G.; Huang, C.; Luo, M. C.; Zheng, J. Study of Molecular Weight and chain Braching Architectures of Natural Rubber. *Appl. Polym. Symp.* **2016**, *133*, 43975.
- (16) Miranda, M. C. R.; Borges, F. A.; Barros, N. R.; Santos Filho, N. A.; Mendonça, R. J.; Herculano, R. D.; Cilli, E. M. Evaluation of Peptides Release Using a Natural Rubber Latex Biomembrane as a Carrier. *Amino Acids* **2018**, *50*, 503–511.
- (17) Dias Murbach, H.; Jaques Ogawa, G.; Azevedo Borges, F.; Romeiro Miranda, M. C.; Lopes, R.; Roberto de Barros, N.; Guedes Mazalli, A. V.; Gonçalves da Silva, R.; Ferreira Cinman, J. L.; de Camargo Drago, B.; Donizetti Herculano, R. Ciprofloxacin Release Using Natural Rubber Latex Membranes as Carrier. *Int. J. Biomater.* **2014**, *2014*, 157952.
- (18) Tian, X.; Han, S.; Zhuang, Q.; Bian, H.; Li, S.; Zhang, C.; Wang, C.; Han, W. Surface Modification of Staple Carbon Fiber by Dopamine to Reinforce Natural Latex Composite. *Polymers* **2020**, *12*, 988.
- (19) Abera, G.; Woldeyes, B.; Demash, H. D.; Miyake, G. The Effect of Plasticizers on Thermoplastic Starch Films Developed from the Indigenous Ethiopian Tuber Crop Anchote (*Coccinia Abyssinica*) Starch. *Int. J. Biol. Macromol.* **2020**, *155*, 581–587.
- (20) Cobos, M.; González, B.; Fernández, M. J.; Fernández, M. D. Study on the Effect of Graphene and Glycerol Plasticizer on the Properties of Chitosan-Graphene Nanocomposites Via in Situ Green Chemical Reduction of Graphene Oxide. *Int. J. Biol. Macromol.* **2018**, *114*, 599–613.
- (21) Barros, N. R.; Ahadian, S.; Tebon, P.; Rudge, M. V. C.; Barbosa, A. M. P.; Herculano, R. D. Highly Absorptive Dressing Composed of Natural Latex Loaded with Alginate for Exudate Control and Healing of Diabetic Wounds. *Mater. Sci. Eng., C* **2021**, *119*, 111589.
- (22) Mbituyimana, B.; Mao, L.; Hu, S.; Ullah, M. W.; Chen, K.; Fu, L.; Zhao, W.; Shi, Z.; Yang, G. Bacterial Cellulose/Glycolic Acid/Glycerol Composite Membrane as a System to Deliver Glycolic Acid for Anti-aging Treatment. *J. Bioresour. Bioprod.* **2021**, *6*, 129–141.
- (23) Motoyama, T.; Katsuumi, Y.; Sasakura, H.; Nakamura, T.; Suzuki, H.; Tsuchiya, K.; Akamatsu, M.; Sakai, K.; Sakai, H. Preparation of Highly Stable Oil-in-Water Emulsions with High Ethanol Content Using Polyglycerol Monofatty Acid Esters as Emulsifiers. *J. Oleo Sci.* **2022**, *71*, 829–837.
- (24) Muniz, K. L.; Dias, F. J.; Coutinho-Netto, J.; Calzzani, R. A.; Iyomasa, M. M.; Sousa, L. G.; Santos, T. T.; Teles, O.; Watanabe, I. S.; Fazan, V. P.; Issa, J. P. Properties of the Tibialis Anterior Muscle after Treatment with Laser Therapy and Natural Latex Protein Following Sciatic Nerve Crush. *Muscle Nerve* **2015**, *52*, 869–875.
- (25) Lima, B.; Ricci, M.; Garro, A.; Juhász, T.; Szigyártó, I. C.; Papp, Z. I.; Feresin, G.; Garcia de la Torre, J.; Lopez Cascales, J.; Fülöp, L.; Beke-Somfai, T.; Enriz, R. D. New Short Cationic Antibacterial Peptides. Synthesis, Biological Activity and Mechanism of Action. *Biochim. Biophys. Acta, Biomembr.* **2021**, *1863*, 183665.
- (26) Suteewong, T.; Wongprecha, J.; Polpanich, D.; Jangpatarapongsa, K.; Kaewsaneha, C.; Tangboriboonrat, P. PMMA Particles Coated with Chitosan-silver Nanoparticles as a Dual Antibacterial Modifier for Natural Rubber Latex Films. *Colloids Surf., B* **2019**, *174*, 544–552.

- (27) Rončević, T.; Gerdol, M.; Mardrossian, M.; Maleš, M.; Cvjetan, S.; Benincasa, M.; Maravić, A.; Gajski, G.; Krce, L.; Aviani, I.; Hrabar, J.; Trumbić, Ž.; Derks, M.; Pallavicini, A.; Weingarth, M.; Zoranić, L.; Tossi, A.; Mladineo, I. Anisaxins, Helical Antimicrobial Peptides from Marine Parasites, Kill Resistant Bacteria by Lipid Extraction and Membrane Disruption. *Acta Biomater.* **2022**, *146*, 131–144.
- (28) Wang, T.; Wang, C.; Zheng, S.; Qu, G.; Feng, Z.; Shang, J.; Cheng, Y.; He, N. Insight into the Mechanism of Internalization of the Cell-Penetrating Carrier Peptide Pep-1 by Conformational Analysis. *J. Biomed. Nanotechnol.* **2020**, *16*, 1135–1143.
- (29) Abbasi, A. R.; Sohail, M.; Minhas, M. U.; Khaliq, T.; Kousar, M.; Khan, S.; Hussain, Z.; Munir, A. Bioinspired Sodium Alginate Based Thermosensitive Hydrogel Membranes for Accelerated Wound Healing. *Int. J. Biol. Macromol.* **2020**, *155*, 751–765.
- (30) Sun, L.; Sun, J.; Chen, L.; Niu, P.; Yang, X.; Guo, Y. Preparation and Characterization of Chitosan Film Incorporated with Thinned Young Apple Polyphenols as an Active Packaging Material. *Carbohydr. Polym.* **2017**, *163*, 81–91.
- (31) Ghasemlou, M.; Khodaiyan, F.; Oromiehie, A. Rheological and structural characterisation of film-forming solutions and biodegradable edible film made from kefir as affected by various plasticizer types. *Int. J. Biol. Macromol.* **2011**, *49*, 814–821.
- (32) Zhao, F.; Tian, Y.; Wang, H.; Liu, J.; Han, X.; Yang, Z. Development of a Biotinylated Broad-specificity Single-chain Variable Fragment Antibody and a Sensitive Immunoassay for Detection of Organophosphorus Pesticides. *Anal. Bioanal. Chem.* **2016**, *408*, 6423–6430.
- (33) Bang, Y.; Obaid, M.; Jang, M.; Lee, J.; Lim, J.; Kim, I. S. Influence of Bore Fluid Composition on the Physicochemical Properties and Performance of Hollow Fiber Membranes for Ultrafiltration. *Chemosphere* **2020**, *259*, 127467.
- (34) Lin, C. C.; Chiu, J. Y. A Novel  $\gamma$ -PGA Composite Gellan Membrane Containing Glycerol for Guided Bone Regeneration. *Mater. Sci. Eng., C* **2021**, *118*, 111404.
- (35) Qian, Y.; Deng, S.; Cong, Z.; Zhang, H.; Lu, Z.; Shao, N.; Bhatti, S. A.; Zhou, C.; Cheng, J.; Gellman, S. H.; Liu, R. Secondary Amine Pendant  $\beta$ -Peptide Polymers Displaying Potent Antibacterial Activity and Promising Therapeutic Potential in Treating MRSA-Induced Wound Infections and Keratitis. *J. Am. Chem. Soc.* **2022**, *144*, 1690–1699.
- (36) Madhyastha, H.; Madhyastha, R.; Thakur, A.; Kentaro, S.; Dev, A.; Singh, S.; Chandrashekarappa, R. B.; Kumar, H.; Acevedo, O.; Nakajima, Y.; Daima, H. K.; Aradhya, A.; Nagaraj, P. N.; Maruyama, M. c-Phycocyanin Primed Silver Nano Conjugates: Studies on Red Blood Cell Stress Resilience Mechanism. *Colloids Surf., B* **2020**, *194*, 111211.
- (37) Sänglerlaub, S.; Kucukpinar, E.; Müller, K. Desiccant Films Made of Low-Density Polyethylene with Dispersed Silica Gel-Water Vapor Absorption, Permeability ( $H_2O$ ,  $N_2$ ,  $O_2$ ,  $CO_2$ ), and Mechanical Properties. *Materials* **2019**, *12*, 2304.
- (38) Park, E.; Long, S. A.; Seth, A. K.; Geringer, M.; Xu, W.; Chavez-Munoz, C.; Leung, K.; Hong, S. J.; Galiano, R. D.; Mustoe, T. A. The Use of Desiccation to Treat Staphylococcus Aureus Biofilm-infected Wounds. *Wound. Repair. Regen.* **2016**, *24*, 394–401.
- (39) de Barros, N. R.; Romeiro Miranda, M. C.; Borges, F. A.; de Mendonca, R. J.; Cilli, E. M.; Herculano, R. D. Oxytocin Sustained Release Using Natural Rubber Latex Membranes. *Int. J. Pept. Res. Ther.* **2016**, *22*, 435–444.
- (40) Li, C.; Zhu, J.; Zhou, M.; Zhang, S.; He, X. Investigation on Water Vapor Adsorption of Silica-Phosphonium Ionic Liquids Hybrid Material. *Materials* **2019**, *12*, 1782.
- (41) Silva, T. V. D.; de Barros, N. R.; Costa-Orlandi, C. B.; Tanaka, J. L.; Moro, L. G.; Pegorin, G. S.; Oliveira, K. S.; Mendes-Gianinni, M. J.; Fusco-Almeida, A. M.; Herculano, R. D. Voriconazole-natural Latex Dressings for Treating Infected Candida spp. Skin Ulcers. *Future Microbiol.* **2020**, *15*, 1439–1452.
- (42) Gontijo de Melo, P.; Fornazier Borges, M.; Afonso Ferreira, J.; Vicente Barbosa Silva, M.; Ruggiero, R. Bio-Based Cellulose Acetate Films Reinforced with Lignin and Glycerol. *Int. J. Mol. Sci.* **2018**, *19*, 1143.
- (43) Gong, X.; Liu, T.; Zhang, H.; Liu, Y.; Boluk, Y. Release of Cellulose Nanocrystal Particles from Natural Rubber Latex Composites into Immersed Aqueous Media. *ACS Appl. Bio Mater.* **2021**, *4*, 1413–1423.
- (44) Chen, S.; Gong, X.; Tan, H.; Liu, Y.; He, L.; Ouyang, J. Study of the Noncovalent Interactions Between Phenolic Acid and Lysozyme by Cold Spray Ionization Mass Spectrometry (CSI-MS), Multi-spectroscopic and Molecular Docking Approaches. *Talanta* **2020**, *211*, 120762.
- (45) Riyajan, S. A.; Sasithornsonti, Y.; Phinyocheep, P. Green Natural Rubber-g-modified Starch for Controlling Urea Release. *Carbohydr. Polym.* **2012**, *89*, 251–258.
- (46) Cazón, P.; Vázquez, M.; Velazquez, G. Composite Films with UV-Barrier Properties of Bacterial Cellulose with Glycerol and Poly(vinyl alcohol): Puncture Properties, Solubility, and Swelling Degree. *Biomacromolecules* **2019**, *20*, 3115–3125.
- (47) Wang, W.; Feng, X.; Du, Y.; Liu, C.; Pang, X.; Jiang, K.; Wang, X.; Liu, Y. Synthesis of Novel Pinocembrin Amino Acid Derivatives and Their Antiaging Effect on Caenorhabditis Elegans Via the Modulating DAF-16/FOXO. *Drug Des., Dev. Ther.* **2021**, *15*, 4177–4193.
- (48) Zhan, Y. H.; Wei, Y. C.; Tian, J. J.; Gao, Y. Y.; Luo, M. C.; Liao, S. Effect of Protein on the Thermogenesis Performance of Natural Rubber Matrix. *Sci. Rep.* **2020**, *10*, 16417.
- (49) Rose, G. D.; Harris, J. K.; McCann, G. D.; Weishuhn, J. M.; Schmidt, D. L. Rapid Gel-like Latex Film Formation Through Controlled Ionic Coacervation of Latex Polymer Particles Containing Strong Cationic and Protonated Weak Acid Functionalities. *Langmuir* **2005**, *21*, 1192–1200.
- (50) Preece, D.; Hong Ng, T.; Tong, H. K.; Lewis, R.; Carré, M. J. The Effects of Chlorination, Thickness, and Moisture on Glove Donning Efficiency. *Ergonomics* **2021**, *64*, 1205–1216.
- (51) Dron, S. M.; Paulis, M. Tracking Hydroplasticization by DSC: Movement of Water Domains Bound to Poly(Meth)Acrylates During Latex Film Formation. *Polymers* **2020**, *12*, 2500.
- (52) Sun, J.; Kroeger, J. L.; Markowitz, J. Introduction to Multiparametric Flow Cytometry and Analysis of High-Dimensional Data. *Methods Mol. Biol.* **2021**, *2194*, 239–253.
- (53) Llavenera, M.; Mislei, B.; Blanco-Prieto, O.; Baldassarro, V. A.; Mateo-Otero, Y.; Spinaci, M.; Yeste, M.; Bucci, D. Assessment of Sperm Mitochondrial Activity by Flow Cytometry and Fluorescent Microscopy: a Comparative Study of Mitochondrial Fluorescent Probes in Bovine Spermatozoa. *Reprod., Fertil. Dev.* **2022**, *34*, 679–688.